Monthly Notices of the ROYAL ASTRONOMICAL SOCIETY

MNRAS **445,** 3345–3351 (2014) doi:10.1093/mnras/stu2006

Improved and expanded measurements of transition probabilities in UV Ar II spectral lines

M. T. Belmonte,[1★] S. Djurović,[2] R. J. Peláez,[3] J. A. Aparicio[1] and S. Mar[1]

[1]*Departamento de Física Teórica, Atómica y Óptica, Universidad de Valladolid, Paseo de Belén 7, E-47011 Valladolid, Spain*
[2]*Department of Physics, Faculty of Sciences, University of Novi Sad, Trg Dositeja Obradovića 4, 21000 Novi Sad, Serbia*
[3]*Laser Processing Group, Instituto de Óptica, CSIC, Serrano 121, E-28006 Madrid, Spain*

Accepted 2014 September 19. Received 2014 September 18; in original form 2014 August 20

ABSTRACT

Transition probabilities have a significant interest in the astrophysical field. The aim of this experiment is to extend the present data base of measured Ar II transition probabilities to the ultraviolet (UV) region and to improve the quality of some of the already existing data. Despite all the efforts made to assemble an accurate set of transition probabilities (A_{ki}), some of the data recommended by the National Institute of Standards and Technology (NIST) for Ar II spectral lines in the UV region have uncertainties around 50 per cent. We measured relative intensities of spectral lines emitted from a low-pressure-pulsed discharge lamp which generates an argon plasma. Excitation temperatures of 19 000–22 000 K are determined from the Boltzmann-plot of 11 Ar II spectral lines for which accurate A_{ki} data are available from the literature. The transition probabilities of these 11 spectral lines were used for calculating new A_{ki}-values. Electron densities (N_e) of 3.5–9.0 × 10^{22} m^{-3} are determined by two-wavelength interferometry method. The measurements yield to a collection of 43 atomic transition probabilities of Ar II lines in the spectral region of 294–386 nm, 11 of which are new, at least up to the authors knowledge, and 22 improved A_{ki}-values for which the existing data in the literature have uncertainties around 50 per cent. Comparison with previous data shows how our measurements have good agreement with the most accurate A_{ki}-values from the bibliography, whereas some of the values recommended by NIST present a significant disagreement.

Key words: Atomic data – Line: profiles – Plasmas – methods: laboratory: atomic.

1 INTRODUCTION

Knowledge of atomic parameters such as the transition probability is of great importance, not only in the theoretical field, but also in the diagnostics of any radiation emitting source, as conventional lamps, lasers, industrial plasmas, fusion or in astrophysics. This fact becomes more relevant for the ionized atoms due to the absence of accurate experimental data from the literature, as is clear from the consultation of the National Institute of Standards and Technology (NIST) data base. Argon plasmas have been extensively studied over the last fifty years due to their desirable characteristics (Wiese 1988) and the suitability of their spectral lines to work as a tool for plasma diagnostics, particularly for temperature determination (Behringer & Thoma 1976). However, despite all the efforts made to assemble an accurate set of transition probabilities (Vujnović & Wiese 1992), some of the data recommended by Kramida et al. (2014) for Ar II spectral lines in the (ultraviolet) UV region have uncertainties of around 50 per cent (Rudko & Tang 1967).

The determination of radiative transition probabilities or oscillator strengths on argon is of common interest in astrophysics. The analysis of the high-resolution stellar spectra is now available in order to estimate the stellar abundances. Weak stellar absorption lines lie on the linear part of the curve growth and hence they have line strengths that are very sensitive to the element abundance. Thus, UV spectral lines of Ar II have been used in the determination of these parameters in B-type stars like γ Peg, HR 1350, 8 Cygni, η Lyrae, Orion B stars (Keenan et al. 1990; Adelman 1998; Lanz et al. 2008). Transition probabilities have contributed to the estimation of abundances in the solar atmosphere, which is quite important for modelling the evolution of the terrestrial and Venusian atmospheres (Lodders 2008). In the field of astronomical instrumentation, UV spectral lines of Ar II have been identified in ThAr lamps. These hollow cathode lamps have become the standard for wavelength calibration of astronomical spectrographs. Wavelength accuracy determines the precision of the radial velocity measurements, and currently there is a great interest in optimizing their precision e.g. radial velocity searches of extrasolar planets or the study of the variability of fundamental constants (Lovis & Pepe

★ E-mail: teruca@opt.uva.es

2007; Murphy et al. 2007). On the other hand, radiometric calibrations of astrophysical instrumentation in the UV and visible range are based on reference Ar I and Ar II branching ratios. In the last decade great effort has been done to provide *f*-values for interpreting the UV and VUV observations made with the *Hubble Space Telescope* (Fedchak & Lawler 2001).

Nowadays, NIST data base (Kramida et al. 2014) is a worldwide reference data base for transition probability data. This work tries to analyse the self-consistency of the A_{ki}-values proposed by NIST for Ar II in the spectral interval 294–386 nm. This paper reports reliable and new transition probabilities for UV Ar II spectral lines, extending much further the experimental work performed by Aparicio, Gigosos & Mar (1997) in our laboratory, where transition probabilities of Ar II lines in the region 360–750 nm were measured. In this experiment, we have measured 43 ionized argon spectral lines in the UV region, yielding 11 new A_{ki}-values for which there are no previous available experimental data, at least up to the authors' knowledge. The method used is based on the measurement of relative intensities of spectral lines emitted from a low-pressure-pulsed discharge lamp which generates an argon plasma with electron densities of 3.5–9.0 × 10^{22} m^{-3} and temperatures of 19 000–22 000 K. The values of the new transition probabilities are obtained by using 11 spectral lines whose A_{ki}-values are already well established in the literature.

2 EXPERIMENTAL METHOD

2.1 Set-up

The experimental set-up shown in Fig. 1 has been described in detail in previous articles (Gigosos et al. 1994) and therefore, only the most relevant aspects will be summarized here for completeness. Also, more specific details corresponding to the present experiment have been reported by Djurovic et al. (2011). Measurements were carried out using a low-pressure-pulsed plasma source.

The plasma was produced inside a cylindrical tube of Pyrex, 175 mm in length and 19 mm in interior diameter. Argon at a pressure of 500 Pa was continuously flowing at a rate of 1 cm^3 min^{-1}. The pressure of argon was adjusted to obtain minimal self-absorption and maximal intensity. The lamp has been designed to avoid sputtering as much as possible. The plasmas were created by

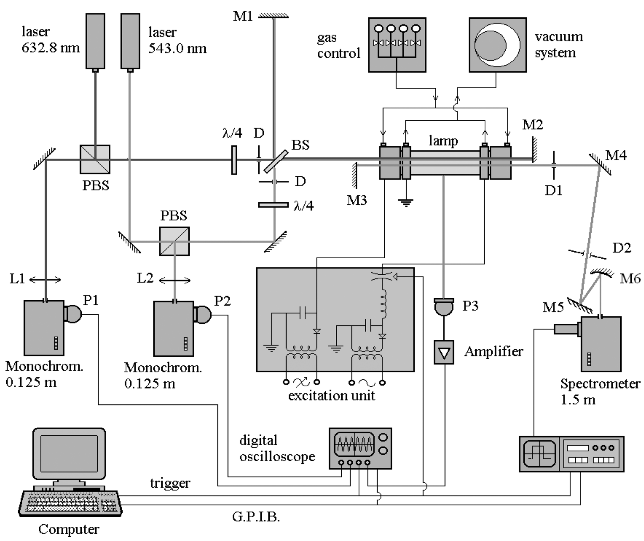

Figure 1. Experimental arrangement.

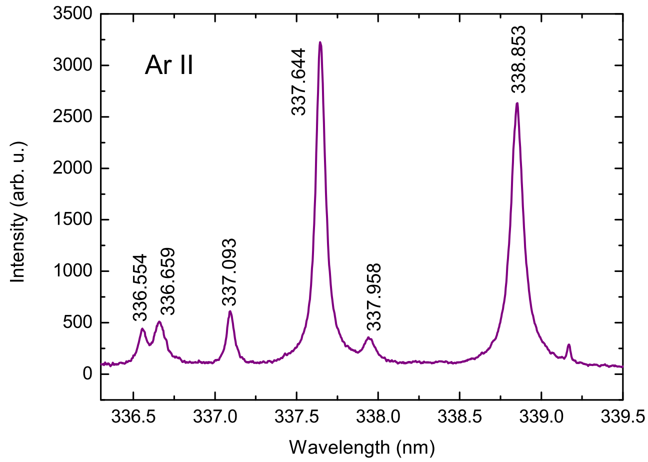

Figure 2. Ar II spectrum at the instant 50 μs of the plasma life.

discharging a capacitor bank of 20 μF charged up to 7.5 kV. The gas in the tube was preionized by a continuous current of several mA in order to ensure plasma reproducibility. In these conditions, the plasma emission lasted for 150 μs. Self-absorption was checked by means of a mirror placed behind the discharge tube (M3 in Fig. 1). Spectroscopic and interferometric end-on measurements have been made simultaneously during the plasma life, and have been taken 2 mm off the lamp axis from symmetrical positions referred to it. The high-axial homogeneity and the very good cylindrical symmetry of electron density and temperature in this lamp (del Val et al. 1998) allow this.

Light emitted from the plasma was limited by two diaphragms and focused by a concave mirror on to the entrance slit of a Jobin–Yvon monochromator (1.5 m focal length, 2400 lines mm^{-1} UV holographic grating). An intensified charge coupled device (ICCD) camera was placed at the exit plane of the monochromator. The slit width of 35 μm was selected in order to obtain the best compromise between the intensity and the resolution. The spectrometer was calibrated in wavelength with uncertainty less than 1 per cent. One of the recorded argon spectrum is shown in Fig. 2. Previous measurements of the spectral transmittance of the windows closing the tube lead us to change them every 800 discharges, in order to reduce the optical transmittance loss to values under 5 per cent at the wavelengths considered in this work. The electrodes were cleaned and polished several times during the experiment. In total 1500 discharges were made.

An incandescent calibrated lamp and a deuterium lamp were used to obtain the spectrometer's transmittance for all wavelengths of interest and for all ICCD channels. The halogen incandescent lamp was calibrated from another incandescent lamp primarily calibrated in NIST with uncertainty around 1.5 per cent. The deuterium lamp (Hamamatsu L6566) was calibrated by the manufacturer who provides a similar uncertainty. The uncertainty of our spectrometer's transmittance function is estimated lower than 4 per cent. The spectral lines were recorded at five different instants from 40 to 120 μs after the beginning of the discharge. All lines were registered in the first order of diffraction. The exposure time was 5 μs. For each instant, 10 different runs were recorded. Three profiles were recorded with and seven without the self-absorption control mirror. The averages and statistical deviations of each group of spectra are calculated in order to increase the signal-to-noise ratio. This statistical deviation is below 5 per cent in more than 95 per cent of the measured spectral intervals. From the comparison of these averaged spectra, we can also check and correct the self-absorption effects and reconstruct the profiles when possible.

The reconstructed spectra were fitted to sums of Lorentzian functions which represent the spectral line profiles and a linear function which represents the continuum emission. The fitting procedure used provides the line intensity, centre, position, and line half-width. The deviations between the experimental profiles and the fitted functions are always lower than 1.5 per cent. Asymmetry was negligible for the Ar II lines. The area under the profile is considered as the relative line intensity used to calculate the transition probabilities. A first selection of suitable Ar II spectral lines is made by excluding all those with some of the following problems: unreliable identification, low intensity, very self-absorbed profiles or highly overlapped spectral lines.

2.2 Plasma diagnostics

The electron density was determined by using a two-wavelength interferometry method (de la Rosa García et al. 1990; Aparicio et al. 1998). The lamp is placed in one of the arms of a Twyman–Green interferometer simultaneously illuminated with two He–Ne lasers (543.5 and 632.8 nm). The laser beams used for interferometric measurements were directed along the discharge tube 2 mm off the tube axis symmetrically with respect to the direction of spectroscopic observations. The influence of heavy particles on variations in the plasma refractive index is eliminated by using this technique. Measured electron densities in this work were in the range 3.5–9.0 × 10^{22} m^{-3}. The experimental error in N_e was estimated to be lower than 10 per cent.

The ionized argon excitation temperature was determined by using the Boltzmann-plot technique (Lochte-Holtgreven 1968) for 11 Ar II spectral lines for which the transition probabilities were well known, all of them belonging to the spectral interval 379–405 nm. An example is shown in Fig. 3. The transition probabilities of these lines were taken from the compilation performed by Vujnović & Wiese (1992) and from Aparicio et al. (1997), see Table 1.

The temperatures obtained were in the range of 19 000–22 000 K. Statistical uncertainties for the excitation temperature are estimated to be lower than 15 per cent. For the electron densities and temperatures considered in this work, calculations carried out by using Griem's criteria (Griem 1963, 1964, 1997) establish that the Ar II energy level scheme is in a partial local thermodynamic equilibrium for levels above 19 eV, which is corroborated by the linear behaviour shown by the Boltzmann-plot (R^2=0.97) within the interval of the energy levels considered (see Fig. 3). Temporal evolution of these plasma parameters is shown in Fig. 4.

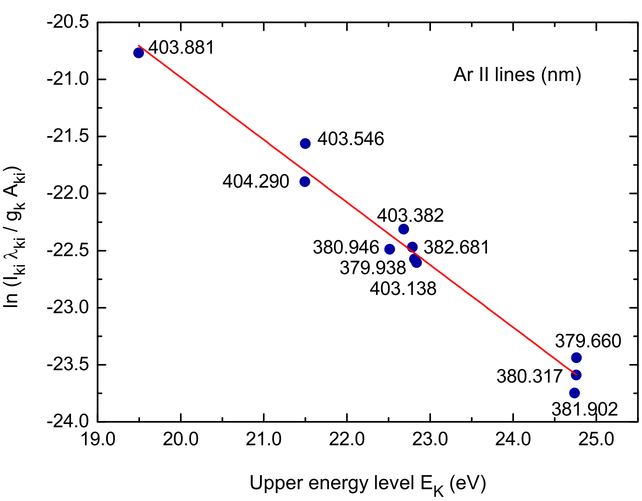

Figure 3. Example of Ar II Boltzmann-plot corresponding to the plasma life instant 50 µs.

3 EXPERIMENTAL RESULTS AND DISCUSSION

Once we obtained the values of *y*-intercept and slope from the Boltzmann-plot for each of the five instants of measurement, we calculated the absolute transition probabilities for the studied spectral lines using their upper energy level and the intensity of each of these lines. We obtained five A_{ki}-values for each line, one per each instant of the plasma life. The average is the proposed value (A_{TW}). In order to perform the Boltzmann-plot, we chose lines for which the transition probabilities are well known. The interval of the upper energy levels considered is 19–25 eV. It is important to remark that all the measured spectral lines, except for two, have upper energy levels within this interval. These two Ar II lines have upper energy levels around 25.5 eV. This also guarantees the validity of the procedure employed to calculate the transition probabilities in this work.

Table 1 shows the measured transition probabilities of the Ar II lines used for the determination of the excitation temperature. We considered 11 Ar II lines from 4s–4p, 3d–4p, 4p–5s, and 4p–4d transitions. In the first three columns the transitions, multiplets, and wavelengths (Kramida et al. 2014) are given. The next four columns contain A_{TW}-values in units of 10^8 s^{-1}, experimental uncertainties (U_{TW}) in percentage, the transition probabilities taken from the bibliography (A_{Ref}), and their corresponding uncertainties (U_{Ref}). The last column gives the bibliographic references from which the A_{Ref}-values were taken. The criteria to select the reference data was to use the data from Vujnović & Wiese (1992)-VW when they exist and their uncertainty was qualified as B in Kramida et al. (2014). In the other cases, data from Aparicio et al. (1997)-AGM were taken. The letter B means that the uncertainty takes values in the range 8–10 per cent, whereas the uncertainty given for Aparicio et al. (1997) data is the square root of the different squared statistical errors provided by the author.

Table 2 shows all the measured transitions. The table is organized in the same way as Table 1. The fourth and fifth columns contain the measured A_{TW}-values of Ar II in units of 10^8 s^{-1} and their estimated uncertainty (U_{TW}) For the comparison, available experimental data A_{Ref} from Vujnović & Wiese (1992)-VW, Rudko & Tang (1967)-RT, Behringer & Thoma (1976)-BT, García & Campos (1985)-GC, and Pellerin et al. (1997)-PMDC are given in column sixth. The seventh column gives their uncertainties U_{Ref}. For VW and RT data, two estimations of the uncertainty are shown. The first value corresponds to the one proposed by the authors in percentage, whereas the second one is the qualifying letter assigned by Kramida et al. (2014). This qualifying letter is always B for data compiled by Vujnović & Wiese (1992) and D for those provided by Rudko & Tang (1967) and later compiled by Wiese, Smith & Miles (1969). In this data base, B corresponds to uncertainties between 8 and 10 per cent, C between 19 and 25 per cent, and D between 41 and 50 per cent. Some theoretical data from Statz et al. (1965)-SHKTK and Luyken (1972)-L are also included in the Table 2 and marked with an asterisk. In all cases, Luyken (1972) data contain two different values which correspond to different ways of calculations. The eighth column contains the A_{Ref}/A_{TW} ratios.

Table 1. Transition probabilities of the Ar II lines used for the determination of the excitation temperature. The references Vujnović & Wiese (1992) and Aparicio et al. (1997) are denoted as VW and AGM, respectively.

Transition	Multiplet	Wavelength (nm)	$A_{\rm TW}$ (10^8 s^{-1})	$U_{\rm TW}$ (per cent)	$A_{\rm Ref}$ (10^8 s^{-1})	$U_{\rm Ref}$ (per cent)	Ref
(^{3}P)3d–(^{3}P)4p	$^4D_{5/2}-^4D^o_{7/2}$	403.880	0.01	14	0.012	10	VW
(^{1}D)4s–(^{1}D)4p	$^2D_{3/2}-^2D^o_{5/2}$	403.546	0.05	16	0.044	10	VW
	$^2D_{3/2}-^2D^o_{3/2}$	404.289	0.39	45	0.406	13	VW
(^{3}P)4p–(^{3}P)5s	$^4P^o_{3/2}-^4P_{5/2}$	380.946	0.31	12	0.339	11	AGM
(^{3}P)4p–(^{3}P)5s	$^4D^o_{3/2}-^4P_{1/2}$	403.381	0.83	14	0.775	11	AGM
(^{3}P)4p–(^{3}P)4d	$^4D^o_{5/2}-^4D_{3/2}$	379.938	0.22	13	0.213	11	AGM
	$^4D^o_{5/2}-^4D_{5/2}$	382.681	0.30	15	0.281	11	VW
(^{3}P)4p–(^{3}P)4d	$^2D^o_{3/2}-^4D_{1/2}$	403.138	0.07	60	0.075	14	VW
(^{1}D)4p–(^{1}D)4d	$^2D^o_{3/2}-^2D_{5/2}$	379.659	0.18	23	0.148	11	AGM
	$^2D^o_{5/2}-^2D_{5/2}$	380.317	0.89	12	0.876	11	AGM
(^{1}D)4p–(^{1}D)4d	$^2D^o_{3/2}-^2P_{3/2}$	381.902	0.15	49	0.166	12	AGM

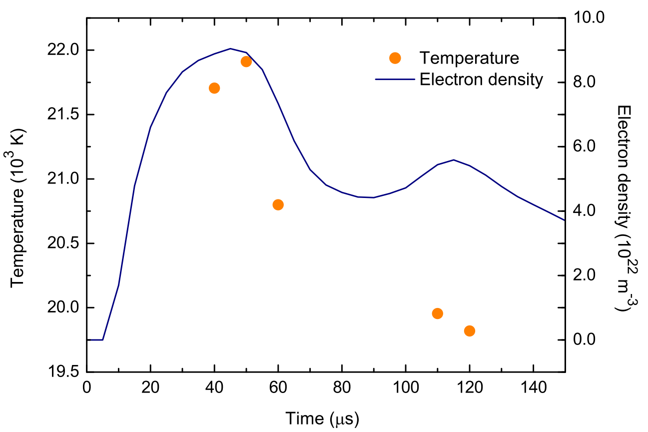

Figure 4. Electron density and temperature evolution in the course of the plasma life.

Following the recommendation made by Vujnović & Wiese (1992), we have paid very careful attention to the estimation of the uncertainty for each of the $A_{\rm TW}$-values. In order to accomplish this task in a consistent and objective manner, we have estimated the uncertainty of each line by taking into account the following aspects.

(a) Standard deviation (σ): it is the standard deviation of the $A_{\rm TW}$-value.

(b) Self-absorption coefficient of the spectral lines (SA): it is the fraction that is necessary to add in order to reconstruct the spectral line of interest. For each line, this coefficient is obtained from the ratio between the increment in the peak intensity due to the reconstruction procedure and this peak intensity on the original profile (Aparicio 1996). When there are not self-absorption effects, the increment is null and consequently this SA coefficient is also null. We have excluded from our results all the Ar II lines whose SA is greater than 0.2.

(c) Background-peak (BP): ratio between the background intensity and the maximum height of the line.

(d) Overlap with the adjacent left ($O_{\rm L}$) or right ($O_{\rm R}$) line: this quantity is given by the next expression:

$$O_i = \frac{w + w_i}{d}\frac{I_i}{I} \tag{1}$$

where i represents left (L) or right (R), w and w_i are the half-widths of the line under study and the adjacent lines (left or right), respectively, and d is the distance between the peaks of the line under study and the adjacent one. The second factor contains the ratio between the intensity of the adjacent line (I_i) and the intensity of the studied line (I). The uncertainty $U_{\rm TW}$ of each spectral line, in percentage, has been calculated with the next mathematical expression that takes into account each of the aspects discussed previously:

$$U_{\rm TW}(\text{per cent}) = 100\sqrt{\sigma^2 + (2({\rm SA})^2)^2 + \left(\frac{\rm BP}{2}\right)^2 + \left(\frac{O_{\rm L}}{20}\right)^2 + \left(\frac{O_{\rm R}}{20}\right)^2}. \tag{2}$$

In general, the equation (2) tends to overestimate the uncertainty. Only spectral lines whose $U_{\rm TW}$ is lower than 60 per cent have been included in Table 2, except for two, 326.899 nm (84 per cent) and 367.326 nm (70 per cent). In these cases, the new values have been considered relevant due to the absence of previous data. We obtained the lowest uncertainty for the intense and well-isolated lines, whereas the highest uncertainties were obtained in cases where the lines had poor intensities or the profiles, in spite of being well defined, were distorted due to the closeness of the neighbouring lines.

A detailed analysis of the $A_{\rm TW}$ and $A_{\rm Ref}$-values reveals a systematic inconsistency between some of the data given by Kramida et al. (2014) and ours. Figs 5(a) and (b) compare the transition probability values taken from Vujnović & Wiese (1992) and from Rudko & Tang (1967), respectively, henceforth $A_{\rm VW}$ and $A_{\rm RT}$, with those measured in this experiment. As can be seen from Fig. 5(a), the $A_{\rm VW}$-values show very good agreement with $A_{\rm TW}$. The linear regression fit has a y-intercept of 0.028 ± 0.016 and a slope of 0.999 ± 0.036. It is possible to observe how the $A_{\rm ki}$-values in Fig. 5(a) are randomly distributed along the unit-slope line, giving a R^2 value of 0.985. As is shown in Fig. 5(b), the linear regression fit for $A_{\rm RT}$-values has a y-intercept of −0.040 ± 0.087 and a slope of 2.204 ± 0.170 with an R^2 value of 0.848, which shows that the $A_{\rm RT}$-values are 2.2 times larger than $A_{\rm TW}$ on average.

Some further analysis can be made by upper energy levels. Only the multiplet $^4P^o$–^4P from the transition 4p–4d contains enough spectral lines with transition probabilities measured in this work as well as by other authors. Fig. 6 (a) shows again the good agreement between VW and TW data. It is important to remark that, in case of the comparison with RT data, the linear behaviour is even improved (R^2=0.990) and the y-intercept is null within its error bar. Both $A_{\rm TW}$ and $A_{\rm VW}$ data are related with $A_{\rm RT}$ data simply by a factor. Regarding the multiplets with the upper level (^{3}P)4d^{2}P, Fig. 7 shows

Table 2. Ar II UV transition probabilities measured in this experiment, A_{TW}, and the available data of other authors, A_{Ref}. The experimental references are denoted as: Vujnović & Wiese (1992)-VW, Rudko & Tang (1967)-RT, Behringer & Thoma (1976)-BT, García & Campos (1985)-GC, and Pellerin et al. (1997)-PMDC. Theoretical references are denoted as: Statz et al. (1965)-SHKTK and Luyken (1972)-L. Theoretical data in A_{Ref} column are followed by *. Transitions and multiplets appear in the same order as in Kramida et al. (2014).

Transition	Multiplet	Wavelength (nm)	A_{TW} (10^8 s^{-1})	U_{TW} (per cent)	A_{Ref} (10^8 s^{-1})	U_{Ref} (per cent)	Ref	A_{Ref}/A_{TW}
$(^3P)4s–(^3P)4p$	$^4P_{5/2}–^2P^o_{3/2}$	384.541	0.010	21	0.002*		SHKTK	0.20
					0.016	22, C	VW	1.60
					0.0091	41, D	RT	0.91
					0.0134*		L	1.34
					0.0088*		L	0.88
$(^3P)4s–(^1D)4p$	$^2P_{3/2}–^2P^o_{3/2}$	294.289	0.42	33	0.53	11, B	VW	1.26
					0.453	12, D	RT	1.08
					0.252	14	GC	0.60
	$^2P_{1/2}–^2P^o_{3/2}$	303.351	0.073	11	0.099	11, B	VW	1.41
					0.0876	12, D	RT	1.25
					0.0807*		L	1.15
					0.0341*		L	0.49
					0.088	15	BT	1.26
					0.077	12	GC	1.10
$(^3P)3d–(^1D)4p$	$^2P_{3/2}–^2P^o_{1/2}$	368.254	0.034	45	0.017	14, B	VW	0.57
					0.00165	8, D	RT	0.06
					0.0395*		L	1.32
					0.0088*		L	0.29
$(^3P)4p–(^3P)5s$	$^4P^o_{1/2}–^4P_{1/2}$	366.960	0.09	17	0.126	8, D	RT	1.40
	$^4P^o_{5/2}–^4P_{3/2}$	367.827	0.17	12	0.254	32, D	RT	1.49
$(^3P)4p–(^3P)4d$	$^4P^o_{5/2}–^4F_{3/2}$	319.423	0.086	12	0.236	36, D	RT	2.62
	$^4P^o_{1/2}–^4F_{3/2}$	326.357	0.13	11	0.155	15, B	VW	1.19
					0.348	36, D	RT	2.68
					0.127	15	BT	0.98
	$^4P^o_{5/2}–^4F_{7/2}$	326.899	0.002	84				
	$^4P^o_{5/2}–^4P_{5/2}$	313.902	0.49	18	0.52	31, C	VW	1.06
					1.00	27, D	RT	2.04
	$^4P^o_{3/2}–^4P_{5/2}$	316.967	0.43	18	0.49	32, C	VW	1.14
					0.817	27, D	RT	1.90
					0.435	15	BT	1.01
	$^4P^o_{5/2}–^4P_{3/2}$	318.104	0.36	12	0.37	30, C	VW	1.03
					0.627	21, D	RT	1.74
					0.372	15	BT	1.03
$(^3P)4p–(^3P)4d$	$^4P^o_{3/2}–^4P_{1/2}$	324.369	1.07	11	1.056	31, C	VW	0.98
					1.99	26, D	RT	1.86
					0.937	15	BT	0.87
	$^4P^o_{1/2}–^4P_{3/2}$	324.980	0.60	14	0.63	31, C	VW	1.05
					1.00	21, D	RT	1.67
					0.621	15	BT	1.04
	$^4P^o_{1/2}–^4P_{1/2}$	328.170	0.41	11	0.42	31, C	VW	1.02
					0.733	26, D	RT	1.79
					0.393	15	BT	0.96
	$^4D^o_{3/2}–^4D_{1/2}$	384.152	0.19	12	0.269	14, B	VW	1.42
					0.267	19, D	RT	1.41
					0.2455	10	PMDC	1.29
	$^4D^o_{5/2}–^4D_{7/2}$	384.473	0.049	17	0.048	15, B	VW	0.96
					0.0474	28, D	RT	0.95
$(^3P)4p–(^1D)3d$	$^4D^o_{3/2}–^2S_{1/2}$	385.614	0.066	18				
$(^3P)4p–(^3P)4d$	$^2D^o_{3/2}–^2P_{3/2}$	320.432	0.24	12	0.402	53, D	RT	1.68
	$^2D^o_{3/2}–^2P_{1/2}$	327.332	0.20	16	0.371	6, D	RT	1.86
	$^2D^o_{5/2}–^2D_{5/2}$	295.539	0.19	13				
	$^2D^o_{3/2}–^2D_{5/2}$	301.448	0.039	19	0.043	15	BT	1.08
	$^2P^o_{3/2}–^4F_{3/2}$	383.017	0.042	27				
	$^2P^o_{3/2}–^2F_{5/2}$	365.528	0.37	13	0.232	26, D	RT	0.63
	$^2P^o_{3/2}–^2P_{3/2}$	329.364	0.59	17	1.73	53, D	RT	2.93
	$^2P^o_{1/2}–^2P_{1/2}$	330.723	1.43	11	3.35	6, D	RT	2.34

Table 2 – *continued*

Transition	Multiplet	Wavelength (nm)	A_{TW} (10^8 s^{-1})	U_{TW} (per cent)	A_{Ref} (10^8 s^{-1})	U_{Ref} (per cent)	Ref	A_{Ref}/A_{TW}
	$^2P^o_{3/2}-^2P_{1/2}$	336.658	0.24	15	0.409	6, D	RT	1.70
	$^2S^o_{1/2}-^2P_{3/2}$	338.853	0.81	12	1.91	53, D	RT	2.36
	$^2S^o_{1/2}-^2D_{3/2}$	316.137	0.35	45	1.83	56, D	RT	5.23
(^{1}D)3d–($^3P_2$)4f	$^2F_{5/2}-^2[3]^o_{7/2}$	316.529	0.038	27				
	$^2F_{7/2}-^2[3]^o_{7/2}$	318.617	0.02	33				
(^{1}D)3d–($^3P_1$)4f	$^2F_{5/2}-^2[4]^o_{7/2}$	304.608	0.095	15				
	$^2F_{7/2}-^2[4]^o_{9/2}$	306.689	0.086	14				
(^{1}D)4p–(^{1}D)4d	$^2F^o_{5/2}-^2F_{5/2}$	335.092	0.90	13	1.48	16, D	RT	1.64
	$^2F^o_{7/2}-^2F_{5/2}$	336.552	0.075	18	0.131	16, D	RT	1.64
	$^2F^o_{7/2}-^2F_{7/2}$	337.644	0.74	13	1.49	2, D	RT	2.01
	$^2P^o_{3/2}-^2P_{3/2}$	366.044	0.73	11	2.22	22, D	RT	3.04
	$^2P^o_{3/2}-^2P_{1/2}$	367.101	0.23	31	0.709	D	RT	3.08
	$^2P^o_{1/2}-^2D_{3/2}$	368.006	0.59	19	1.15	28, D	RT	1.95
(^{1}D)4p–(^{3}P)6s	$^2P^o_{1/2}-^2P_{3/2}$	367.326	0.11	70				
(^{1}D)4p–(^{1}D)4d	$^2P^o_{3/2}-^2S_{1/2}$	302.675	1.03	21				
(^{1}D)3d–($^3P_1$)5f	$^2D_{3/2}-^2[2]^o_{5/2}$	300.296	0.062	28				
(^{1}D)4p – (^{1}D)4d	$^2D^o_{5/2}-^2P_{3/2}$	382.567	0.33	55	0.756	22, D	RT	2.29
					0.7600	35	PMDC	2.30

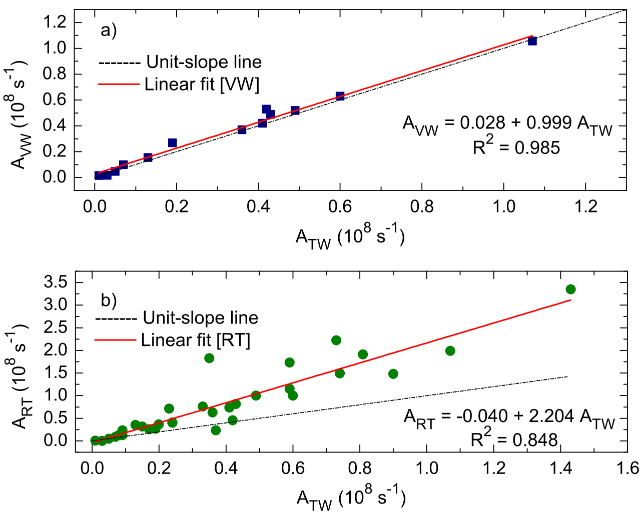

Figure 5. Comparison of the transition probabilities measured in this experiment A_{TW} with (a) those from Vujnović & Wiese (1992) compilation, and (b) those from Rudko & Tang (1967).

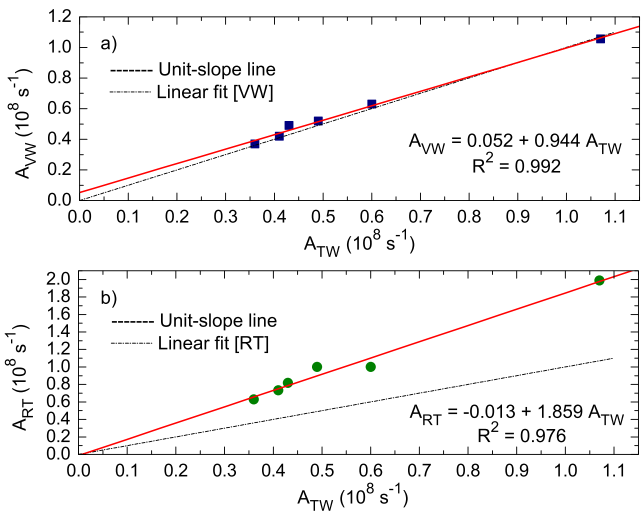

Figure 6. Comparison of the transition probabilities measured in this experiment A_{TW} for the multiplet $^4P^o$–^{4}P from the transition 4p–4d with (a) those from Vujnović & Wiese (1992) compilation, and (b) those from Rudko & Tang (1967).

the comparison between A_{RT} and ours. In this case, the line of fit has a *y*-intercept of -0.092 ± 0.124 and a slope of 2.491 ± 0.170 with an R^2 value of 0.978, once more higher than that obtained in Fig. 5 (b). The A_{RT}-values for this multiplet are systematically 2.5 times larger than A_{TW} on average. All these analyses agree with some of the ideas suggested by Vujnović & Wiese (1992), according to which atomic lifetime values for 4p and 4d levels from Rudko & Tang (1967) are underestimated. These discrepancies with some of the data from Rudko & Tang (1967) are not contemplated in the erratum from Rudko & Tang (1968).

Finally, our data show very good agreement with the experimental data from Behringer & Thoma (1976). Unfortunately, there are only eight results from these authors, five of them belong to the multiplet 4d^{4}P and are in good agreement with Vujnović & Wiese (1992) data.

4 CONCLUSIONS

This paper reports reliable and new A_{ki}-values for UV Ar II spectral lines extending much further the experimental work performed by Aparicio et al. (1997) in our laboratory. In this experiment, we have measured 43 ionized argon spectral lines in the ultraviolet region from 294 to 386 nm, yielding 11 new transition probabilities for which there are no previous available experimental data, at least up to the authors' knowledge, and 22 A_{ki}-values for which the existing data have uncertainties around 50 per cent.

We have paid special attention to all the possible sources of experimental uncertainty that are likely to affect our transition probability measurements. In addition, the measured A_{ki}-values have been carefully studied and compared with the existing data, finding a significant lack of self-consistency in the Kramida et al. (2014) data base worth analysing.

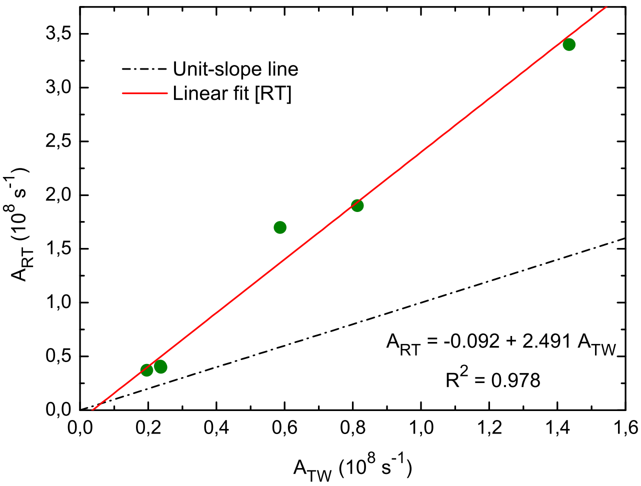

Figure 7. Comparison of A_{TW} with A_{RT} for lines coming from the multiplets with the upper level (^{3}P)4d^{2}P.

Finally, the results given here can extend the present data base of measured Ar II transition probabilities to the UV region and many of them could be useful in refining new theoretical models.

ACKNOWLEDGEMENTS

We thank S González for his work on the experimental device. MTB thanks the University of Valladolid for her PhD scholarship and RJP acknowledges the grant JCI-2012_13034 from the Juan de la Cierva programme. SD thanks the Ministry of Education, Science, and Technological Development of the Republic of Serbia for support via Project 171014.

REFERENCES

Adelman S. J., 1998, MNRAS, 296, 856
Aparicio J. A., 1996, PhD thesis, Universidad de Valladolid
Aparicio J. A., Gigosos M. A., Mar S., 1997, J. Phys. B, 30, 3141
Aparicio J. A., Pérez C., del Val J. A., Gigosos M. A., de la Rosa M. I., Mar S., 1998, J. Phys. B, 31, 4909
Behringer K., Thoma P., 1976, J. Quant. Spectrosc. Radiat. Transfer, 16, 605
de la Rosa García M. I., Pérez García Ma . C., de Frutos Baraja A. M., Mar Sardaña S., 1990, Phys. Rev. A, 42, 7389
del Val J. A., Mar S., Gigosos M. A., de la Rosa I., Pérez C., González V., 1998, Japan. J. Appl. Phys., 37, 4177
Djurovic S., Mar S., Peláez R. J., Aparicio J. A., 2011, MNRAS, 414, 1389
Fedchak J. A., Lawler J. E., 2001, J. Quant. Spectrosc. Radiat. Transfer, 68, 483
García G., Campos J., 1985, J. Quant. Spectrosc. Radiat. Transfer, 34, 85
Gigosos M. A., Mar S., Pérez C., de La Rosa I., 1994, Phys. Rev. E, 49, 1575
Griem H. R., 1963, Phys. Rev., 131, 1170
Griem H. R., 1964, Plasma Spectroscopy. McGraw-Hill, New York
Griem H. R., 1997, Principles of Plasma Spectroscopy. Cambridge Univ. Press, Cambridge
Keenan F. P., Bates B., Dufton P. L., Holmgren D. E., Gilheany S., 1990, ApJ. 348, 322
Lanz T., Cunha K., Holtzman J., Hubeny I., 2008, ApJ. 678, 1342
Lochte-Holtgreven W., 1968, in Lochte-Holtgreven W, ed., Plasma Diagnostics. North-Holland, Amsterdam, p. 135
Lodders K., 2008, ApJ, 674, 607
Lovis C., Pepe F., 2007, A&A, 468, 1115
Luyken B. F. J., 1972, Physica, 60, 432
Murphy M. T., Tzanavaris P., Webb J. K., Lovis C., 2007, MNRAS, 378, 221
Kramida A., Ralchenko Yu., Reader J., NIST ASD Team, 2014, NIST Atomic Spectra Database (version 5.2), Available at: http://physics.nist.gov/asd
Pellerin S., Musiol K., Dzierzega K., Chapelle J., 1997, J. Quant. Spectrosc. Radiat. Transfer, 57, 359
Rudko R. I., Tang C. L., 1967, J. Appl. Phys., 38, 4731
Rudko R. I., Tang C. L., 1968, J. Appl. Phys., 39, 4046
Statz H., Horrigan F. A., Koozekanani S. H., Tang C. L., Koster G. F., 1965, J. Appl. Phys., 36, 2278
Vujnović V., Wiese W. L., 1992, J. Phys. Chem. Ref. Data, 21, 919
Wiese W. L., 1988, J. Quant. Spectrosc. Radiat. Transfer, 40, 421
Wiese W. L., Smith M. V., Miles B. M., 1969, Atomic Transition Probabilities, Vol. II, Sodium Through Calcium, NSRDS-NBS 22. National Stand. Ref. Ser., Nat. Bur. Stand., Washington, DC

This paper has been typeset from a TEX/LATEX file prepared by the author.